

## NUMERIC RECONSTRUCTION OF 2D CELLULAR ACTOMYOSIN NETWORK FROM SUBSTRATE DISPLACEMENT

W. S. Nishitani\*, R. C. Carbonari\*\* and A. M. Alencar\*

\*Universidade de São Paulo, Physics Institute, São Paulo, SP, Brazil

\*\* Universidade Federal do ABC, Santo André, SP, Brazil

e-mail: wagnersn@if.usp.br

**Abstract:** One of the fundamental structural elements of the cell is the cytoskeleton. Along with myosin, actin microfilaments are responsible for cellular contractions. The study of these filaments is important because their organization may be related to pathological changes in myocardial tissue. Cytoskeleton is also related to mechanotransduction, the translation of mechanical signals into biochemical ones by the cell. Due to the complexity of factors involved in mechanotransduction, numerical modeling of the cytoskeleton may contribute to a better understanding of mechanical cues in cellular activities. The establishment of a systematic method for cytoskeleton reconstruction of a cell under investigation may accelerate substantially the development of mathematical models. In this work, it was developed a systematic method for the reconstruction of an actomyosin topology from the displacement exerted by the cell on a flexible substrate. It is an inverse problem, solved with a Topology Optimization Method (TOM), where an actomyosin distribution is found in order to reproduce experimental displacements generated by the cell. These displacements were obtained by Traction Force Microscopy (TFM). The structure resulting from TOM was compared to the actin structures observed experimentally. This method could be considered a phenomenological approach to TFM.

**Keywords:** Traction Force Microscopy, cell mechanics, actin, Topology Optimization Method, Finite Element Method.

### Introduction

One of the fundamental structural elements of the cell is the cytoskeleton. It is composed by microtubules, intermediate filaments and microfilaments. Microfilaments are composed by F-actin, filaments produced by polymerization of G-actin. Along with myosin, microfilaments are responsible for cellular contraction. The study of these filaments could be important because their organization may be related to pathological changes in myocardial tissue [1], as extracellular matrix (ECM) microstructure are related to alignment of cells and cytoskeleton morphology [2-4]. Cytoskeleton is also related to mechanotransduction [5]. Mechanotransduction is the translation of mechanical signals into biochemical ones by the cell. The mechanotransduction of mechanical signals from the ECM in adherent cells depends on integrins, which form

focal adhesions. Integrins are proteins responsible for anchoring cells to the ECM and consequently for the transmission of forces applied by the cells to their substrate [5].

Due to the complexity of factors involved in mechanotransduction, numerical modeling of the cytoskeleton may contribute to a better understanding of mechanical cues in cellular activities. The utilization of simplified models may clarify which factors are really essential and which have only a marginal influence. The establishment of a systematic method for cytoskeleton reconstruction of a cell under investigation may accelerate substantially the development of mathematical models. Systematic methods of reconstruction may also allow a faster comparison of experimental data with numerical results, accelerating mathematical model validation [6].

In this work, it was developed a systematic method for the reconstruction of actomyosin topology from the displacement exerted by the cell on a flexible substrate. It is an inverse problem as it may be analogous to reconstructing a traction field from its displacement.

The inverse nature of the problem justifies the use of the Topology Optimization Method (TOM), whose applications include an electric impedance tomography [7], for example. TOM consists of an iterative application of an optimization method followed by an analysis method to obtain an optimal distribution of material in a fixed domain. Thus, this method was used to produce an actomyosin distribution of the cytoskeleton from a flexible substrate displacement generated by the cell. These displacements were obtained experimentally by Traction Force Microscopy (TFM). The structure resulting from TOM was compared to the actin structures observed experimentally. This method could be considered a phenomenological approach to TFM.

## Materials and methods

**Cell culture** – The cells used in the experiments were Rabbit Aortic Smooth Muscle (RASM), kindly provided by Prof. José Eduardo Krieger (Instituto do Coração da Faculdade de Medicina da Universidade de São Paulo, InCor-HC-FMUSP). They were cultured in T-25 flasks (Corning, 430639) at 37°C in 5% CO<sub>2</sub>. The growth medium was composed by Dulbecco's Modified Eagle Medium (DMEM) supplemented with 10% Fetal Bovine Serum (FBS) and 1% Antibiotic-Antimycotic (Gibco, 15240). To visualize actin fibers, the cells were transfected with pCMV LifeAct-TagGFP2 plasmid (ibidi, 60101), a GFP-attached actin marker developed by Riedl et al. [8; 9], kindly provided by Prof. Marinilce Fagundes dos Santos (Instituto de Ciências Biomédicas da Universidade de São Paulo, ICB-USP).

**Flexible substrate** – The flexible substrates were made of polyacrylamide gel, whose preparation was based on protocols already established [10]. The substrates had a Young modulus of 4.8 kPa and were made with Acrylamide at 7.5%, Bis at 0.054%. Their thickness was about 50 μm with a very thin layer of polyacrylamide with 0.2 μm fluorescent microbeads (Molecular Probes, F-8810) [11]. The substrate surface was then activated with Sulfo-SANPAH (Thermo Scientific, 22589), according to the supplier protocol, and incubated overnight at 4°C with 200 μl of collagen I (BD, rat-tail) at 0.2 mg/ml (0.035 mg/cm<sup>2</sup>).

**Traction Force Microscopy** – The displacement field generated by the cell attached to a flexible substrate was obtained as part of a Traction Force Microscopy experiment, already described in the literature [12], consisting of acquiring images of the substrate fluorescent microbeads before and after the cells were removed with a Trypsin-EDTA treatment. The postprocessing of images to obtain the displacement and traction field was done with a plugin for ImageJ developed by Tseng et al. [13], which is an approach similar to the one used by Butler et al. [14] with additional regularization. Images from the marked actin were also acquired to verify the reconstruction results.

**Numerical reconstruction of actin-myosin** – The algorithm was implemented with linear Finite Element Method (MEF) for the displacement analysis. The substrate was modeled with a single layer of 8-node brick elements with the bottom surface constrained for no displacement. The actomyosin domain was modeled with 4-node bidimensional rectangular elements. Their nodal degrees of freedom were directly coupled to  $x$  and  $y$  degrees of freedom from the substrate top surface nodes. The present TOM implementation optimizes the material density  $\rho$  and angle of contraction  $\theta$  of the actomyosin structure over a bidimensional domain of rectangular elements, as shown in Figure 1.

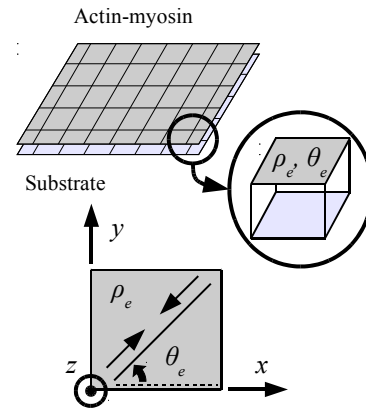


Figure 1: Domains of actin-myosin and substrate. Actomyosin element, rigidly linked to the substrate, and its variables (density  $\rho_e$  and angle of contraction  $\theta_e$ ).

The topology generated by TOM minimizes  $\Delta D$ , the nodal displacement differences squared between the generated topology and experimental displacement fields, which is the objective function for this optimization problem:

$$\min_{\rho, \theta} \Delta D = \sum_{n=0}^{N_{nodes}} (u_n - \tilde{u}_n)^2 \quad (1)$$

where  $N_{nodes}$  is the number of nodes in the actomyosin domain, and  $u_n$  and  $\tilde{u}_n$  are the topology and experimental displacement of the node  $n$ .

The actomyosin density is represented by the material interpolation model “Simple Isotropic Material with Penalization” (SIMP) [15], varying between zero and one continuously.

The formulation used for linear elastic bidimensional elements for plane stress or tridimensional elements was described by Zienkiewicz and Taylor [16]. The actomyosin contraction was modeled by Sen et al. [17] as an isotropic initial stress of the elements. In this work, contraction is also modeled as an initial stress determined by an initial strain composed by  $x$  and  $y$  components according to the angle  $\theta_e$  of each element. Contraction of the actomyosin structure was modulated by: 1) changing the material stiffness, through its Young modulus and thickness of the bidimensional elements; 2) changing the initial strain. Actomyosin contraction is the result of the equilibrium between the initially stressed actomyosin and substrate elements. An infinitely high stiffness of the actomyosin elements would cause a significant displacement even for densities  $\rho_e$  near zero, making it more difficult to visualize intermediate densities. Thus, it is important to test actomyosin parameters with material properties initially closer to the substrate.

The routine was implemented in Matlab R2009 (Mathworks), with the optimizer Globally Convergent Method of Moving Asymptotes (GCMMA) [18].

## Results

The TFM experiment yielded a brightfield and three fluorescent images: one of the marked actin and two of the substrate markers (microbeads). The postprocessing resulted in the displacement and traction fields. The brightfield, marked actin and postprocessing results are shown in Figure 2.

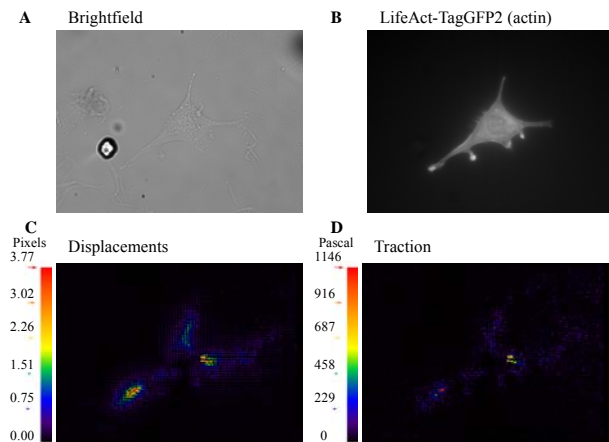


Figure 2: TFM experiment results, with A) brightfield and B) marked actin images, along with C) displacement and D) traction fields.

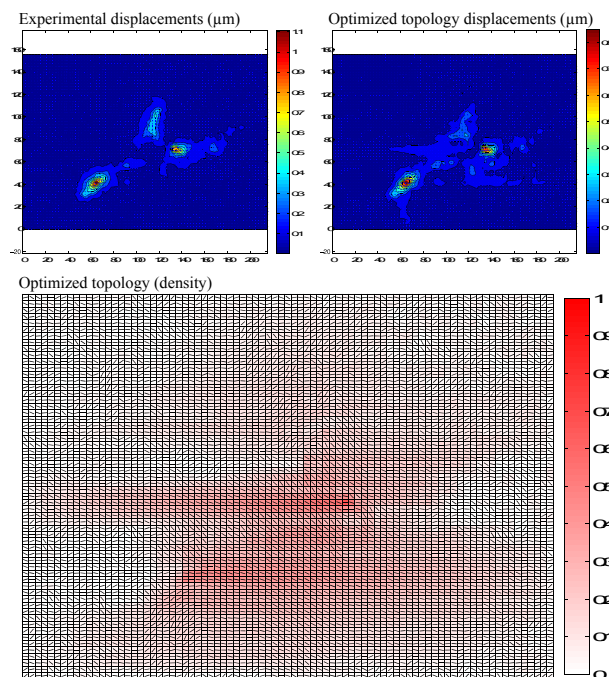


Figure 3: Numerical reconstruction of actomyosin structure, and comparison between experimental and reconstructed displacement fields.

For the numerical reconstruction of the actomyosin topology, the Poisson's ratio for the actomyosin material was 0.3 (compressible) [19; 20] and, for the substrate, 0.48 (almost incompressible) [21]. After some tests, the optimal Young modulus and initial strain for the

actomyosin material was 76.8 kPa, sixteen times the substrate Young modulus, and 80%, respectively. The thickness for the actomyosin elements was 1  $\mu\text{m}$  and, for the substrate, 0.5  $\mu\text{m}$ . The optimized topology, along with its displacement field compared to the experimental data, are shown in Figure 3. As a quantification of the quality of the reconstruction, the squared displacement differences  $\Delta D$  was compared to the sum of experimental squared nodal displacements. In this case,  $\Delta D$  was 11.24  $\mu\text{m}^2$ , 27.5% of the sum of experimental squared nodal displacements (40.87  $\mu\text{m}^2$ ).

## Discussion

The choice of element geometry and model of contraction had a significant impact in the routine capability to minimize the displacement differences. The use of rectangular elements for the actomyosin domain allowed a better representation of contractions in  $x$  and  $y$  directions relative to intermediate angles. The composition of an intermediate angle in terms of these orthogonal directions led to an identical contraction for the negative of that angle, which is something to be aware when interpreting the results. Also, the contraction becomes isotropic for angles of  $45^\circ$  and  $-45^\circ$ .

Overall, the routine was capable of reproducing the main features of the experimental displacements. The denser actomyosin regions in the optimized topology correlated to regions covered by the cell. Regarding the actomyosin fiber orientation, the algorithm tends to orient them in the protrusion directions next to the cell boundary. In the inner regions, the optimized topology tends to contract more isotropically (angles closer to  $45^\circ$  or  $-45^\circ$ ). There are lower density regions in the topology outside the area covered by the cell, which can be explained by one hypothesis of the model. It was assumed that the cells were adhered to the substrate all over their extension because it was considered that the actomyosin domain nodes are directly coupled to the substrate top surface nodes. Thus, regions that are not adhered linking adhered portions of the cytoskeleton were represented by an actomyosin distribution over a larger area, minimizing the sum of squared displacement differences ( $\Delta D$ ).

Some regions of the experimental cell were not represented in the optimized topology, which indicates that the cell is not using them actively to produce substrate displacement. This feature could be useful in studies where the goal is to distinguish functionality among the actomyosin fibers.

The present work, despite considering an uniform initial strain for the actomyosin material model, allows local variations of fiber contractility due to differences in the material density distribution in the optimized topology. Also, the anisotropic nature of the actomyosin initial strain allows preferential contraction directions. Both aspects can contribute to existing models, which considered isotropic contractions over the cytoplasm [17], for example.

As the algorithm targets the network of one particular cell, it utilizes more efficiently the experimental data available by not averaging the cell heterogeneity. In this work, the experimental data of one cell was analyzed to show the algorithm functionality.

## Conclusion

An actomyosin numerical reconstruction routine was implemented with a linear material model for the bidimensional actomyosin elements and tridimensional substrate. The optimized topology reproduced the main features of the experimental data. The present approach extends the literature with a more detailed model of the actomyosin structure, capable of distributing anisotropic material freely, allowing more heterogeneous contractions over the cell extension.

## Acknowledgements

We want to thank Prof. José Eduardo Krieger (Instituto do Coração da Faculdade de Medicina da Universidade de São Paulo, InCor-HC-FMUSP) for providing the RASM cells; Prof. Marinilce Fagundes dos Santos (Instituto de Ciências Biomédicas da Universidade de São Paulo, ICB-USP) for providing the pCMV LifeAct-TagGFP2 plasmid; grant #2012/07907-9, São Paulo Research Foundation (FAPESP); CAPES and CNPq.

## References

- [1] Hiremath, P.; Bauer, M.; Aguirre, A. D.; Cheng, H.-W.; Unno, K.; Patel, R. B.; Harvey, B. W.; Chang, W.-T.; Groarke, J. D.; Liao, R. and others. Identifying Early Changes in Myocardial Microstructure in Hypertensive Heart Disease. *PLoS one*. 2014; 9:e97424.
- [2] Tomasek, J. J.; Gabbiani, G.; Hinz, B.; Chaponnier, C. and Brown, R. A.. Myofibroblasts and mechano-regulation of connective tissue remodelling. *Nature Reviews Molecular Cell Biology*. 2002; 3:349-363.
- [3] Rhee, S. and Grinnell, F.. Fibroblast mechanics in 3D collagen matrices. *Advanced drug delivery reviews*. 2007; 59:1299-1305.
- [4] Fernandez, P. and Bausch, A. R.. The compaction of gels by cells: a case of collective mechanical activity. *Integrative biology*. 2009; 1:252-259.
- [5] Ingber, D. E.. Cellular mechanotransduction: putting all the pieces together again. *FASEB Journal*. 2006; 20:811-827.
- [6] Ghosh, S.; Matsuoka, Y.; Asai, Y.; Hsin, K.-Y. and Kitano, H.. Software for systems biology: from tools to integrated platforms.. *Nature Reviews Genetics*. 2011; 12:821-832.
- [7] Mello, L. A. M.; de Lima, C. R.; Amato, M. B. P.; Lima, R. G. and Silva, E. C. N.. Three-dimensional electrical impedance tomography: a topology optimization approach.. *IEEE Transactions on Biomedical Engineering*. 2008; 55:531-540.
- [8] Riedl, J.; Crevenna, A. H.; Kessenbrock, K.; Yu, J. H.; Neukirchen, D.; Bista, M.; Bradke, F.; Jenne, D.; Holak, T. A.; Werb, Z. and others. Lifeact: a versatile marker to visualize F-actin. *Nature methods*. 2008; 5:605-607.
- [9] Riedl, J.; Flynn, K. C.; Raducanu, A.; Gärtner, F.; Beck, G.; Bösl, M.; Bradke, F.; Massberg, S.; Aszodi, A.; Sixt, M. and others. Lifeact mice for studying F-actin dynamics. *Nature methods*. 2010; 7:168-169.
- [10] Lo, C.-M.; Wang, H.-B.; Dembo, M. and Li Wang, Y.. Cell movement is guided by the rigidity of the substrate. *Biophysical Journal*. 2000; 79:144-152.
- [11] Bridgman, P. C.; Dave, S.; Asnes, C. F.; Tullio, A. N. and Adelstein, R. S.. Myosin IIB is required for growth cone motility. *The Journal of neuroscience : the official journal of the Society for Neuroscience*. 2001; 21:6159-6169.
- [12] Dembo, M. and Wang, Y. L.. Stresses at the cell-to-substrate interface during locomotion of fibroblasts.. *Biophysical Journal*. 1999; 76:2307-2316.
- [13] Tseng, Q.; Duchemin-Pelletier, E.; Deshieri, A.; Bolland, M.; Guillou, H.; Filhol, O. and Théry, M.. Spatial organization of the extracellular matrix regulates cell-cell junction positioning. *Proceedings of the National Academy of Sciences*. 2012; 109:1506-1511.
- [14] Butler, J. P.; Tolić-Nørrelykke, I. M.; Fabry, B. and Fredberg, J. J.. Traction fields, moments, and strain energy that cells exert on their surroundings.. *American Journal of Physiology. Cell Physiology*.. 2002; 282:C595-C605.
- [15] Bendsøe, M. P. and Sigmund, O.. Material interpolation schemes in topology optimization. *Archive of applied mechanics*. 1999; 69:635-654.
- [16] Zienkiewicz, O. C. and Taylor, R. L.. *The finite element method: The basis*. :Butterworth-heinemann; 2000. p. .
- [17] Sen, S.; Engler, A. J. and Discher, D. E.. Matrix strains induced by cells: Computing how far cells can feel.. *Cellular and Molecular Bioengineering*. 2009; 2:39-48.
- [18] Svanberg, K.. A class of globally convergent optimization methods based on conservative convex separable approximations. *SIAM Journal on Optimization*. 2002; 12:555-573.
- [19] Pelletier, V.; Gal, N.; Fournier, P. and Kilfoil, M. L.. Microrheology of microtubule solutions and actin-microtubule composite networks. *Physical review letters*. 2009; 102:188303.
- [20] Das, M. and MacKintosh, F.. Poisson's ratio in composite elastic media with rigid rods. *Physical review letters*. 2010; 105:138102.
- [21] Boudou, T.; Ohayon, J.; Picart, C. and Tracqui, P.. An extended relationship for the characterization of Young's modulus and Poisson's ratio of tunable polyacrylamide gels. *Biorheology*. 2006; 43:721-728.